1 Contact State Segmentation using Particle Filters for Programming by Human Demonstration in Compliant Motion Tasks

Wim Meeussen, Johan Rutgeerts, Klaas Gadeyne, Herman Bruyninckx, and Joris De Schutter

Department of Mechanical Engineering,
Katholieke Universiteit Leuven,
Celestijnenlaan 300B, B-3001 Leuven, Belgium.
wim.meeussen@mech.kuleuven.be
http://mech.kuleuven.be

Abstract. This paper presents a contribution to *programming by human demonstration*, in the context of *compliant motion* task specification for sensor-controlled robot systems that physically interact with the environment. One wants to learn about the geometric parameters of the task and segment the total motion executed by the human into subtasks for the robot that can each be executed with simple compliant motion task specifications. The motion of the human demonstration tool is sensed with a 3D camera, and the interaction with the environment is sensed with a force sensor in the human demonstration tool. Both measurements are uncertain, and do not give direct information about the *geometric* parameters of the contacting surfaces, or about the *contact formations* encountered during the human demonstration. The paper uses a Bayesian Sequential Monte Carlo method (also known as a *particle filter*) to do the simultaneous estimation of the contact formation (discrete information) and the geometric parameters (continuous information). The simultaneous contact formation segmentation and the geometric parameter estimation are helped by the availability of a *contact state graph* of all possible contact formations. The presented approach applies to all compliant motion tasks involving polyhedral objects with a known geometry, where the uncertain geometric parameters are the poses of the objects. The approach has been verified in real world experiments, in which it is able to discriminate in realtime between 245 different contact formations of the contact state graph.

1.1 Introduction

Compliant motion [1] refers to tasks in which an object held by a manipulator moves while maintaining contact with the environment. The force interaction at the contact is used to guide the manipulated object along the surface of the environmental object, to help overcome geometric uncertainties associated with the task. A task specification for a compliant motion task can be obtained using *programming by human demonstration*, where a human demonstrates the desired compliant motion task [2, 3]. The demonstration can be performed in a virtual environment using a haptic device, in the real world by directly interacting with a robot through a master slave system, or, like the example presented in this paper, by observing human motion when the demonstrator directly manipulates the objects in the environment

without the use of a robot. During the demonstration, sensor data about the task is collected. After the demonstration, in an interpretation step, the sensor data is interpreted based on a geometric contact model of the objects, and translated into a path plan of a compliant motion.

Major challenges in the automatic translation from human compliant motion demonstration into a path plan of a compliant motion are: (i) to recognize the *contact formation* to which the human demonstration is currently subjected, (ii) to estimate the geometric parameters of that contact formation (i.e., position of contact point(s), direction of contact normal(s), etc.), and (iii) to detect when exactly the human demonstration execution changes between two contact formations. Even between two simple polyhedral objects, *hundreds* of contact formations are possible, and, hence, hundreds of transitions between neighboring contact formations. Recently Gadeyne et al. [4] developed a *particle filter* [5] to recognize, simultaneously, contact transitions, and estimate geometric pose parameters of a *known* geometric model in an unknown pose. Their approach is able to estimate geometric parameters with a large uncertainty, and simultaneously recognize contact transitions in an experiment consisting of six initially known possible contacts. The low number of possible contacts allows them to use a simple prediction step in the particle filter, in combination with a small number of particles.

This paper generalizes and scales the approach of Gadeyne et al. to cope with *all possible contacts* between two polyhedral objects. To cope with this increased complexity, a more accurate prediction step is used, based on the topological information contained in a contact state graph, [6], and the pose of the contacting objects. This paper also presents efficient algorithms for the pose and consistency measurement equations, allowing the estimators to be used in *realtime*.

The paper is organized as follows. Section 1.2 briefly reviews the concepts of contact formations and the contact state graph. Section 1.3 describes the demonstration tool which is used to collect sensor data during human demonstration in compliant motion. The interpretation of this sensor data, using Bayesian estimation techniques, is covered in Section 1.4. Section 1.5 describes the real world experiments that validate the presented approach. Finally, Section 1.6 contains conclusions and future work.

1.2 Contact Formations and the Contact State Graph

1.2.1 Contact Formations

The notion of *principal contacts* (PCs) was introduced [7] to describe a contact primitive between two surface elements of two polyhedral objects in contact, where a surface element can be a face, an edge or a vertex. Fig. 1.1 shows the six non-degenerate[1] PCs that can be formed between two polyhedral objects. Each non-

[1] The vertex-vertex, vertex-edge and edge-vertex PCs are called degenerate, as it is difficult to achieve a stable contact that includes one of these PCs. Therefore only non-degenerate PCs are considered in this paper.

degenerate PC is associated with a *contact plane*, defined by a contacting face or the two contacting edges at an edge-edge PC.

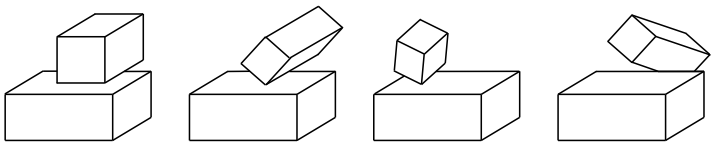

Fig. 1.1. The six possible non-degenerate principal contacts (PCs) between two polyhedral objects.

A general contact state between two objects can be characterized topologically by the set of PCs formed, called a *contact formation* (CF). Each configuration of two objects, i.e. their relative pose in space, compliant to the constraints of a CF, is called a *CF-compliant configuration*, denoted by a pose $\boldsymbol{X}$. Any motion formed by a sequence of CF-compliant configurations is called a *CF-compliant motion*. A homogeneous transformation matrix represents the relative pose of two objects.

A PC can be decomposed into one or more *Elementary Contacts* (ECs), providing a lower level description of the CF. The three types of ECs (face-vertex, vertex-face and edge-edge) are shown in the two examples at the right of Fig. 1.1. An EC is a point contact and is associated with a *contact point* and a *contact normal*.

1.2.2 Contact State Graph

Xiao and Ji developed a divide-and-merge approach [6] to generate a compact, simplified representation of the contact state space between two polyhedral objects, as a *contact state graph* G. In G a node represents a CF, and an arc connecting two nodes represents the adjacency relationship between the CFs of the nodes. Two CFs CF_i and CF_j are adjacent if a compliant motion from a CF_i-compliant configuration to CF_j-compliant configuration exists, which only includes CF_i and CF_j-compliant configurations. Fig. 1.2 shows an example of a contact state graph containing seven different CFs and their adjacency relationships. The approach was implemented to automatically generate a contact state graph that can contain hundreds of contact formations.

1.3 Demonstration Tool

In programing by human demonstration, a task specification for a compliant task involving a manipulated object and its environment is obtained by observing a human demonstrate the desired task. In this research the human demonstrator directly interacts with the manipulated object, using a *demonstration tool* which is mounted onto the manipulated object.

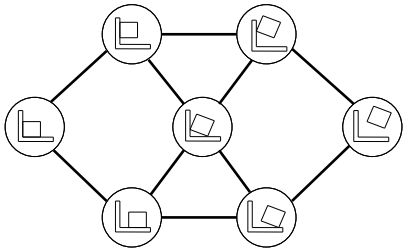

Fig. 1.2. A complete contact state graph shows all possible CFs (nodes) and transitions between neighboring CFs (arcs). While this figure shows a simplified example that only contains 7 CFs, a real contact state graph of two 3-dimensional polyhedral objects contains hundreds of CFs.

1.3.1 Design

The demonstration tool is shown in Fig. 1.3. A handle on top provides an easy grasp for the human demonstrator to manipulate the demonstration tool and the object attached to it. The demonstration tool consists of nine faces, and up to four LED markers can be mounted on each face. The Krypton K600 6D optical system measures the spatial positions of the LED markers, at $100\ [Hz]$, with a volumetric accuracy of $90\ [\mu m]$. Inside the demonstration tool, a *JR3* wrench sensor is mounted between the demonstration tool and the manipulated object, to measure the wrench $\boldsymbol{w}_m$ (linear force and moment) applied by the human demonstrator to the manipulated object. The calibration of the demonstration tool is discussed in [8].

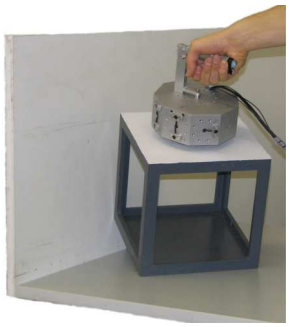

Fig. 1.3. The demonstration tool is manipulated in contact with three perpendicular faces. The Krypton K600 optical system uses three cameras and triangulation algorithms to measure the spacial position of each of the LED markers on the demonstration tool.

1.3.2 Estimate Pose and Twist from LED markers

While the wrench $\boldsymbol{w}_m$ is directly measured by a physical sensor, the pose $\boldsymbol{X}_m$ (position and orientation) and twist $\boldsymbol{t}_m$ (translational and rotational velocity) between the contacting objects are indirectly measured through the positions of the LED markers that are visible to all three camera's. Due to the geometry of the demonstration tool, the maximum number of simultaneously visible LED markers is 12, while at least 4 visible LED markers are needed by our algorithm to extract the pose and twist of the demonstration tool.

Say the number of LED markers visible to all three camera's is $v \geq 4$. Then the camera system measures v positions $\boldsymbol{p}_1^c \dots \boldsymbol{p}_v^c$, relative to the camera (c). The positions of the LED markers $\boldsymbol{p}_1^d \dots \boldsymbol{p}_v^d$ relative to the demonstration tool (d), are known from an initial calibration phase. In a first step, the pose matrix (rotation matrix $\boldsymbol{R}_c^d$ and position vector $\boldsymbol{p}_c^d$) of the demonstration tool is calculated in a minimization problem.

In a second step, this calculated pose is an input to a linear estimation problem to obtain both the demonstration tool's pose $\boldsymbol{X}_m$ and twist $\boldsymbol{t}_m$, based on a constant acceleration model [9]. The Kalman filter is the preferred tool for this linear estimation problem with low uncertainties. The filter uses an 18-dimensional state vector which contains the pose vector $\boldsymbol{x}$ (XYZ position and ZYX Euler angles), the velocity $\dot{\boldsymbol{x}}$ and the acceleration $\ddot{\boldsymbol{x}}$. All three 6-dimensional parameters are estimated from the initially calculated pose. The estimated pose and velocity vector, are converted into the pose $\boldsymbol{X}_m$ and the twist $\boldsymbol{t}_m$.

1.4 Simultaneous Recognition of Contact Formations and Estimation of Geometric Parameters

A compliant motion task can be segmented into a sequence of CFs. At each CF, different contact constraints apply. Therefore, to estimate uncertain geometric parameters of the objects involved in a compliant motion task, the knowledge of the current CF model is required. This means that the estimation problem for compliant motion tasks, consists of two connected sub-problems: the recognition of the (discrete) CF and the estimation of (continuous) geometric parameters.

In this paper particle filters [5] are used to implement this hybrid estimation problem. The particle filter algorithm updates the discrete CF and continuous geometric parameters in a two step approach. In the first step the system model makes a prediction for the next CF and the geometric parameters. In the second step the measurement model corrects this prediction based on sensor data. This section describes the models that are used in the estimation problem.

1.4.1 Hybrid Probability Density Function

A hybrid *probability density function* (PDF) contains both continuous and discrete variables. A time-invariant variable is called a *parameter*, while a time-dependent

variable is called a *state*. The continuous parameters in this paper are called the geometric parameters, and represent the pose of the manipulated object relative to the demonstration tool and the pose of the environmental object relative to a world reference. Note that while the pose of the objects is unknown, their geometry is known. The discrete state in this paper represents the CF at time step k.

1.4.2 System Model – Prediction

The prediction step uses the system model to make a prediction for the hybrid joint density at time step k, given the hybrid joint density at time step $k-1$. Because the geometric parameters are time-invariant, the system model only needs to predict the next CF. The system model expresses the belief in a CF transition from a CF_a at time step $k-1$, to a CF_b at time step k, given the geometric parameters.

To predict the next CF out of hundreds of theoretically possible next CFs, the topological information from the objects' contact state graph is used. The adjacency relationship between CFs, which is defined by arcs connecting CFs in the contact state graph, indicates if a direct transition between two CFs is possible (see Fig. 1.2), which drastically reduces the number of possible next CFs. If two CFs are not adjacent, a transition between them is considered impossible. Between two adjacent CFs a transition is possible, and the closer the two objects are, the more likely this transition will occur. The probability of a transition is calculated similar as for the pose measurement equations, as explained in Section 1.4.3.

1.4.3 Measurement Model – Correction

The correction step uses two measurement models to calculate the hybrid joint density at time step k, given the prediction for the hybrid joint density at time step k. A measurement model represents the belief in a measurement, given the geometric parameters and the CF. This paper uses a model based on the pose measurement $\boldsymbol{X}_m$, and a model based on the wrench and twist measurements $\boldsymbol{w}_m$ and $\boldsymbol{t}_m$. Both models are applied in every correction step.

Contact distance measurement model based on pose measurements The contact distance measurement model expresses that when the manipulated object is in contact with the environmental object, the distance between the objects at the contact ECs should be zero, thereby closing the kinematic chain between the objects. The distance between the objects at non-contact ECs should be greater than zero, expressing that the objects do not penetrate nor contact. A new measurement variable is created by combining the distances at all ECs into one distance vector. The pose measurement model expresses the belief in this new distance measurement variable, which is a nonlinear function of the pose measurement $\boldsymbol{X}_m$ and the geometric parameters.

Calculating the distance at all ECs would be numerically expensive. Therefore, only the distances at ECs directly connected to the predicted CF by an edge are calculated. The distance calculation at the ECs is also helped by the use of spherical

boundary boxes around the elements of the ECs. Only when two boundary boxes intersect, the exact distance at an EC is calculated.

Residue measurement model based on wrench-twist measurements The residue measurement model expresses the consistency between the contact constraints, and the wrench and twist measurements $\boldsymbol{w}_m$ and $\boldsymbol{t}_m$ [10]. The consistency is expressed by a residue vector $\boldsymbol{r}_m$, which contains the part of the measured twist and wrench that is not explained by the first order kinematics of an ideal frictionless contact; it should vanish when the measurements and the model are consistent.

For a given pose and CF, the first order kinematics are represented by a wrench space and a twist space. The wrench space contains all possible wrenches that can be applied between the contacting objects at the current pose, and is spanned by the wrench vectors of $\boldsymbol{W}$. The twist space contains all possible instantaneous twists that maintain the contact, and is spanned by the twist vectors of $\boldsymbol{T}$. Both $\boldsymbol{W}$ and $\boldsymbol{T}$ can be calculated with one *singular value decomposition* (SVD).

The calculation of the residue vector requires the evaluation of two weighted pseudo-inverses, that each require another SVD. This paper presents an algorithm to calculate the residue vector without the pseudo-inverses, by exploiting the orthonormal nature of the matrices $\boldsymbol{W}$ and $\boldsymbol{T}$ obtained from the SVD [11]. The algorithm is valid when choosing diagonal weighting matrices $\boldsymbol{K}_w$ and $\boldsymbol{K}_t$ that are each others inverse. This results in an algorithm with only one single SVD, which reduces the computational cost of the overall filter with 55%.

1.4.4 Software

The presented implementation is capable of processing $90,000$ particles per second, on a $2\ [GHz]$ AMD 64 laptop, sufficient for realtime discrimination between 245 CFs and estimation of uncertain geometrical parameters. The filter algorithms are implemented within the framework offered by the open source C++ Bayesian Filtering Library (BFL) [12]. BFL offers a unifying framework for all recursive Bayesian filters, such as Kalman filters, extended Kalman filters and particle filters. It provides efficient implementations of various filter algorithms.

1.5 Experiments

This section reports on the real world experiment to validate the presented approach. In the experiment, a human demonstrator manipulates a cube through a complex sequence of CFs in an environment consisting of three perpendicular faces, as shown in Fig. 1.3. The particle filter algorithm uses 20.000 particles and processes measurements at $4\ [Hz]$.

1.5.1 Initial Uncertainty

The initial uncertainty on the 12-dimensional continuous geometric parameters, which are the poses of the environmental and manipulated objects, is represented

by uniform distributions. The uniform distributions have a width of $15\ [mm]$ on the x and y positions, and $0.5\ [rad]$ on the roll-pitch-yaw orientations. Only the distribution on the z position has a width of $130\ [mm]$. The discrete state can be any of the 245 possible CFs between the cube and the planes, and there is initially no contact between the objects.

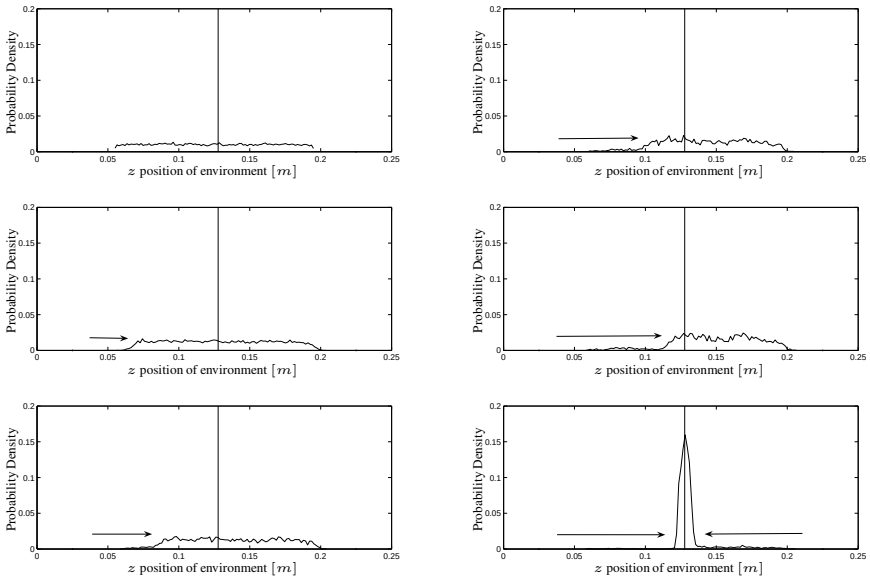

Fig. 1.4. The time evolution of the probability density on the position of a plane, when approaching the plane with a cube.

1.5.2 Approach to First Contact

In the first part of the experiment, the cube has no contact with the environment, and approaches one of the planes of the environment. Fig. 1.4 shows the time evolution of the uncertainty on the z position of the environment. The uncertainty on this position, represented by a histogram, is 1 component of the 12-dimensional continuous parameter; it is obtained by integrating over the 11 other components, for a given CF. The first five sub-figures show the position parameter for the no-contact CF, while the sixth sub-figure shows the position parameter for the first vertex-face CF. Initially the position is represented by a uniform distribution, indicating that there is little knowledge about its value. When the cube approaches the plane, the probability decreases on the left side of the distribution. This shows that the cube

"penetrated" one of the possible positions of the plane without detecting a contact, thus proving that possible position invalid. This evolution continues until the cube makes a vertex-face CF with the plane. The new contact allows accurate estimation of the position of the plane, also decreasing the probability on the right side of the uniform distribution.

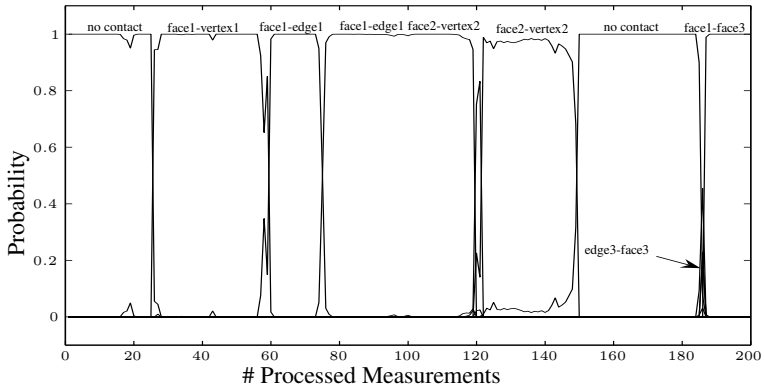

Fig. 1.5. The CF evolution of a human demonstration where a cube is manipulated in contact with two perpendicular faces. The evolution is shown by the probability on each of the CFs.

1.5.3 Sequence of Contact Formations

In the rest of the experiment, the cube is manipulated in contact with the environment, through a complex sequence of CFs. The experiment includes complex CFs and CF transitions, such as adding and removing contact constraints, adding and removing many contact constraints at once, and simultaneous contacts with the two planes. Fig. 1.5 shows the estimated probability on each of the 245 possible CFs. This probability is obtained by integrating over all 12 components of the continuous parameter, for each possible CF. At each time step only a few CFs have a probability greater than zero. The particle filters successfully assign the highest probability to the CF that corresponds to the true CF in the experiment.

1.6 Conclusions

This paper presents a contribution to the task specification process for sensor-controlled robot systems that physically interact with the environment, with a focus on compliant motion tasks. Particle filters are applied to simultaneously estimate the current discrete contact formation out of 245 possible contact formations, and the 12-dimensional continuous geometric parameter, from sensor data gathered during

a human demonstration. The same particle filter algorithms can also be used to process sensor data collected during the execution of a compliant motion task. When processing this data online, during the execution, the estimators can provide feedback to the robot controller about the current CF and estimate geometrical parameters related to the robot manipulator and its environment. The performance of the presented algorithms is sufficient to process all sensor data in realtime. Using the estimators online to provide feedback for the robot controller will be the subject of further research and experiments.

Acknowledgment

All authors gratefully acknowledge the financial support by K.U.Leuven's Concerted Research Action GOA/05/10. The authors also acknowledge Jing Xiao of the university of North Carolina at Charlotte and her research group for providing their software for the automatic generation of a contact state graph.

References

1. J. De Schutter and H. Van Brussel, "Compliant Motion I, II," *Int. J. Robotics Research*, vol. 7, no. 4, pp. 3–33, Aug 1988.
2. H. Asada and H. Izumi, "Automatic program generation from teaching data for the hybrid control of robots," *ITRA*, vol. 5, no. 2, pp. 166–173, 1989.
3. J. Chen, "Constructing task-level assembly strategies in robot programming by demonstration," *Int. J. Robotics Research*, vol. 24, pp. 1073–1085, 2005.
4. K. Gadeyne, T. Lefebvre, and H. Bruyninckx, "Bayesian hybrid model-state estimation applied to simultaneous contact formation recognition and geometrical parameter estimation," *Int. J. Robotics Research*, vol. 24, no. 8, pp. 615–630, 2005.
5. A. Doucet, N. J. Gordon, and V. Krishnamurthy, "Particle Filters for State Estimation of Jump Markov Linear Systems," *IEEE Trans. Signal Processing*, vol. 49, no. 3, pp. 613–624, march 2001.
6. J. Xiao and X. Ji, "On automatic generation of high-level contact state space," *Int. J. Robotics Research*, vol. 20, no. 7, pp. 584–606, 2001.
7. J. Xiao, "Automatic determination of topological contacts in the presence of sensing uncertainty," in *Int. Conf. Robotics and Automation*, Atlanta, GA, 1993, pp. 65–70.
8. J. Rutgeerts, P. Slaets, F. Schillebeeckx, W. Meeussen, B. Stallaert, P. Princen, T. Lefevbre, H. Bruyninckx, and J. De Schutter, "A demonstration tool with Kalman Filter data processing for robot programming by human demonstration," in *Proc. IEEE/RSJ Int. Conf. Int. Robots and Systems*, Edmonton, Canada, 2005, pp. 3918–3923.
9. Y. Bar-Shalom and X. Li, *Estimation and Tracking, Principles, Techniques, and Software*. Artech House, 1993.
10. M. S. Ohwovoriole and B. Roth, "An extension of screw theory," *Trans. ASME J. Mech. Design*, vol. 103, no. 4, pp. 725–735, 1981.
11. W. Meeussen, J. Rutgeerts, K. Gadeyne, H. Bruyninckx, and J. De Schutter, "Contact state segmentation using particle filters for programming by human demonstration in compliant motion tasks," K.U.Leuven, Leuven, Belgium, Tech. Rep., 2006.
12. K. Gadeyne, "BFL: Bayesian Filtering Library," http://people.mech.kuleuven.ac.be/∼kgadeyne/bfl, 2001.